ISSN: 2277-3754
ISO 9001:2008 Certified
International Journal of Engineering and Innovative Technology (IJEIT)
Volume 4, Issue 3, September 2014

Hydrodynamic Characteristics of Channel Contractions

Edward Ching-Ruey, LUO
Doctor of Engineering, Asian Institute of Technology
Assistant Professor Department of Civil Engineering, National Chi-nan University, Nantou, TAIWAN

Abstract*—the design of channel transition from subcritical flow into supercritical one with the manner of typical straight-line channel contractions by the principles of non-uniform flow with a minimum amount of surface disturbance has received the attention of hydraulic engineers. Design for minimum of standing waves, therefore, is the particular goal for flow at supercritical velocities so that economic structures may result. The purpose of this paper is to explore the analytical results of hydrodynamic characteristics of 2-DH contraction flow, such as primary flow velocity profile, profile of turbulent wall shear stress, and profiles of turbulent viscosity coefficient and dispersion coefficient, are derived. Then the shape factor formed as the ratio between the mass displacement thickness and the momentum displacement thickness is calculated to explain the influence on pressure gradient, and friction coefficient. Finally, the 2-DH hydrodynamic characteristics of contraction flow are used to compare with the ones of non-diffuser and expanded flows and the corresponding discussion, conclusions and applications are summarized.

Index Terms—**Contraction flow, turbulence, hydrodynamics, displacement thickness, friction coefficient.**

I. INTRODUCTION

Shallow water flows in channels are of interest in a variety of physical problems. These include river flow through a canyon, river deltas, and canals. Under certain conditions we can get large hydraulic jumps or their moving counterparts bores, in the channel. There are a number of places where these bores are generated in rivers around the world. In shallow flows in natural or man-made channels, contraction geometry is not uncommon. It consists of a more or less uniform channel followed by a contraction of the channel into a nozzle where the width is minimal before the channel suddenly or gradually fans out again. Large variations in water flow discharges through such contracting channels may lead to dramatic changes in the flow state, such as stowage effects with upstream moving surges. Such phenomena do occur when rivers overflow and the water is funneled underneath constricting bridges or through ravines. Flows with one or two oblique hydraulic jumps occur for smaller discharges, e.g., at underpasses for roadside streams or through gates of the storm surge barrier. Similar situations also occur in downslope of the water-laden debris flows, when oversaturated mountain slopes collapse. In this paper, however, we limit ourselves to study the flow states of water flow through an idealized uniform channel and linear contraction as a type for the above-mentioned more complex flow geometries. Froude number of upstream flow and increasing values of the scaled nozzle width defined by the ratio of the upstream channel width and nozzle width will be the significant items. Shallow flows are often assumed to be incompressible and the modeled with the 2D depth-averaged steady-state shallow water equations (2-DH) and a medium specific, determined friction law are considered in this paper.

II. THEORETICAL CONSIDERATION

It is one of the most fundamental phenomenon of study in the field of fluid mechanics with the Newtonian and non-Newtonian flow case. Investigations have been performed in order to understand the incompressible flow downstream of a channel contraction, which is planar and is normal to the direction of the channel wall. 2-DH flow researches into this channel flow allow better understanding of boundary layer separation, re-attachment and recirculation, which are common features in engineering practice. Many turbulence models based on Reynolds-averaged Navier-Stokes equations, such as zero-equation turbulence model, one-equation turbulence model, two-equation turbulence model and Reynolds stress/flux model, have been successfully applied to the simulation of turbulent flows in computational fluid dynamics (CFD). For the depth averaged simulation of river flows, one of the most often used two-equation turbulence models is Rastogi and Rodi's [1] depth-averaged standard k-ε" turbulence model. In the present study, Chen and Kim's [2] presented the non-equilibrium k-ε" turbulence model and Yahkot et al's [3] expressed the RNG k-ε" turbulence model, which are widely used in CFD, are extended to the depth-averaged 2-D simulation of river flows. The depth-integrated continuity and momentum equations of turbulent flow in open channels are:

$$\frac{\partial h}{\partial t}+\frac{\partial(hU)}{\partial x}+\frac{\partial(hV)}{\partial y}=0 \qquad (1)$$

$$\frac{\partial}{\partial x}(HU^2)+\frac{\partial}{\partial y}(HUV)+gH\frac{\partial \xi}{\partial x}+\frac{\tau_{bx}}{\rho}-\frac{\partial(HT_{xx})}{\rho\,\partial x}-\frac{\partial(HT_{xy})}{\rho\,\partial y}=0 \qquad (2)$$

$$\frac{\partial(HUV)}{\partial x}+\frac{\partial(HV^2)}{\partial y}+gH\frac{\partial \xi}{\partial y}+\frac{\tau_{by}}{\rho}-\frac{\partial(HT_{xy})}{\rho\,\partial x}-\frac{\partial(HT_{yy})}{\rho\,\partial y}=0 \qquad (3)$$

Where t is the time; x and y are the horizontal Cartesian coordinates; h is the flow depth; U and V are the depth-averaged flow velocities in x- and y-directions; zs is the water surface elevation; g is the gravitational acceleration; is the density of flow. It should be noted that Eqs. (2) and (3) do

ISSN: 2277-3754
ISO 9001:2008 Certified
International Journal of Engineering and Innovative Technology (IJEIT)
Volume 4, Issue 3, September 2014

not include the dispersion terms that exist due to the vertical non-uniformity of flow velocity. Their effect is assumed to be negligible in this study, but the treatment of these terms has been studied by Flokstra [4], Wu and Wang and others [5]. and the turbulent stresses are determined by Boussinesq's assumption:

$$\tau_{by} = \rho c_f U\sqrt{U^2+V^2} \quad (4)$$

$$\tau_{by} = \rho c_f U\sqrt{U^2+V^2} \quad (5)$$

$$c_f = gn^2/h^{1/3} \quad (6)$$

$$T_{xx} = 2\rho(\nu+\nu_t)\frac{\partial U}{\partial x} - \frac{2}{3}\rho k \quad (7)$$

$$T_{xy} = T_{yx} = \rho(\nu+\nu_t)\left(\frac{\partial U}{\partial y}+\frac{\partial V}{\partial x}\right) \quad (8)$$

$$T_{yy} = 2\rho(\nu+\nu_t)\frac{\partial V}{\partial y} - \frac{2}{3}\rho k \quad (9)$$

Where ν is the kinematic viscosity of water; ν_t is the eddy viscosity due to turbulence; k is the turbulence energy. The k in Eqs. (7), (8) and (9) is dropped when the zero - equation turbulence models are considered.

A. Standard k-ε" Turbulence Model

Rastogi and Rodi [1] established the depth averaged k-ε" turbulence model through depth integrating with the 3-D standard k-ε" model. The eddy viscosity $\nu_t$is calculated by:

$$\nu_t = c_\mu k^2/\varepsilon \quad (10)$$

Where c_μ is an empirical constant? The turbulence energy k and its dissipation rate " are determined with the following model transport equations:

$$\bar{U}\frac{\partial \bar{k}}{\partial x} + \bar{V}\frac{\partial \bar{k}}{\partial x} = \frac{\partial}{\partial x}\left(\frac{\bar{\nu}_t}{\sigma_t}\frac{\partial \bar{k}}{\partial x}\right) + \frac{\partial}{\partial y}\left(\frac{\bar{\nu}_t}{\sigma_t}\frac{\partial \bar{k}}{\partial y}\right) + P_h + P_{kv} - \varepsilon \quad (11)$$

$$\bar{U}\frac{\partial \bar{\varepsilon}}{\partial x} + \bar{V}\frac{\partial \bar{\varepsilon}}{\partial x} = \frac{\partial}{\partial x}\left(\frac{\bar{\nu}_t}{\sigma_\varepsilon}\frac{\partial \bar{\varepsilon}}{\partial x}\right) + \frac{\partial}{\partial y}\left(\frac{\bar{\nu}_t}{\sigma_\varepsilon}\frac{\partial \bar{\varepsilon}}{\partial y}\right) + c_{1\varepsilon}\left(\frac{\bar{\varepsilon}}{\bar{k}}\right)P_h + P_{\varepsilon v} - c_{2\varepsilon}\left(\frac{\bar{\varepsilon}^2}{\bar{k}}\right) \quad (12)$$

Where:

$$P_h = \nu_t|\bar{S}|^2,$$

$$P_{kv} = c_f^{-1/2}U_*^3/h; \qquad P_{\varepsilon v} = c_{\varepsilon\Gamma}c_{\varepsilon 2}c_\mu^{1/2}c_f^{-3/4}U_*^4/h^2;$$

$$c_\mu = 0.09;\ c_{1\varepsilon} = 1.44;\ c_{2\varepsilon} = 1.92;\ c_{\varepsilon\Gamma} = 1.8 \text{ to } 3.6;$$

$$\sigma_k = 1.0;\ \sigma_\varepsilon = 1.3;$$

B. Non-equilibrium k-ε" Turbulence Model

Chen and Kim [2] modified the standard k-ε" turbulence model to consider the non-equilibrium between the generation and dissipation of turbulence. A second time scale of the production range of turbulence kinetic energy spectrum is added to the dissipation rate equation, which results in a functional form of coefficient,

$$c_{\varepsilon 1} = 1.15 + \frac{0.25P_h}{\varepsilon}$$

$$c_\mu = 0.09;\ c_{2\varepsilon} = 1.90;$$

$$\sigma_k = 0.8927;\ \sigma_\varepsilon = 1.15;$$

The modified model was called the non-equilibrium k-ε" turbulence model (Shyy et al [6]) which has been tested in a compressible recirculating flow with improved performance over the standard model. By using Rastogi and Rodi's [1] depth-averaging approach, the depth-averaged non-equilibrium k-ε" model can be derived from the 3-D version. The formulations of k- and ε-equations are still the same as Eqs. (11) and (12), with only the model coefficients being replaced accordingly.

C. RNG k-ε Turbulence Model

Yakhot et al [3] re-derived the "ε-equation (12) using the re-normalized group (RNG) theory. One new term was introduced to take into account the highly anisotropic features, usually associated with regions of large shear, and to modify the viscosity accordingly. This term was claimed to improve the simulation ac-curacy of the RNG k-ε" turbulence model for highly strained flow. By analogy to the above non-equilibrium turbulence model, the depth averaged 2-D RNG k-ε" turbulence model can also be derived, whose k- and "ε-equations are the same as Eqs. (11) and (12), with the new term being included in the coefficient,

$$c_{\varepsilon 1} = 1.42 - \eta\,(1-\eta/\eta 0)/(1+\beta\eta^3)$$

$$\beta = 0.015, \eta = |\bar{S}|\,k/\varepsilon\,, \eta 0 = 4.38$$

$$c_\mu = 0.085, c_{\varepsilon 2} = 1.68, \sigma k = 0.7179, \sigma_\varepsilon = 0.7179$$

D. Boundary Conditions

Near rigid wall boundaries, such as banks and islands, the wall-function approach is employed. By applying the log-law of velocity, the resultant wall shear stress $\vec{\tau}_w$ is related to the flow velocity $\vec{V}_p$ at center P of the control volume close to the wall, by the following relation:

$$\vec{\tau}_w = -\lambda\vec{V}_p \quad (13)$$

$$\lambda = \rho c_\mu^{1/4}k_p^{1/2}\kappa/\ln(Ey_p^+) \quad (14)$$

$$11.6 < y_p^+ < 300$$

$$y_p^+ = \rho c_\mu^{1/4}k_p^{1/2}y_P/\mu, u_* = c_\mu^{1/4}k_p^{1/2} \quad (15)$$

which can be obtained with the assumption of local equilibrium of turbulence (see Rodi [7]). In the zero-equation turbulence models, the turbulence energy k is not solved, hence λ is determined by:

$$\lambda = \rho u_*\kappa/\ln(Ey_p^+), y_p^+ = \rho u_* y_P/\mu \quad (16)$$

In three k-ε" turbulence models, the turbulence generation Ph and the dissipation rate near the wall are determined by,

ISSN: 2277-3754
ISO 9001:2008 Certified
International Journal of Engineering and Innovative Technology (IJEIT)
Volume 4, Issue 3, September 2014

$$P_{h,p} = \tau_w^2/\kappa\mu y_P^+,\ \varepsilon p = c_\mu^{3/4} k_p^{3/2}/\kappa y_P \quad (17)$$

III. ANALYTICAL SOLUTIONS

In Luo [8], the proposed resultant hydrodynamic characteristic equations are derived based on:

Initial condition:

$$P_{kv} = C_k\left(\frac{u_*^3}{h}\right);\quad P_{\varepsilon v} = C_\varepsilon\left(\frac{u_*^4}{h^2}\right) \quad (18)$$

Friction velocity:

$$u_*^2 = C_f\left(\overline{U}^2 + \overline{V}^2\right) \quad (19)$$

$$C_K = \frac{1}{\sqrt{C_f}};\quad C_\varepsilon = \frac{3.6 C_{2\varepsilon}}{C_f^{3/2}}\sqrt{C_\mu} \quad (20)$$

Rough bed coefficient from Manning formula with rough factor, n:

$$C_f = \frac{n^2 g}{h^{1/3}} \quad (21)$$

Local bottom shear stress:

$$\frac{\tau_b}{\rho} = u_*^2 = C_f\left(\overline{U}^2 + \overline{V}^2\right) \quad (22)$$

$$\tau_b = \frac{\rho g}{C_c^2}\left(\overline{U}^2 + \overline{V}^2\right) \quad (23)$$

Bottom shear stress in x- and y-directions:

$$\frac{\tau_{bx}}{\tau_b} = \frac{\overline{U}}{\sqrt{\overline{U}^2 + \overline{V}^2}} \quad and \quad \frac{\tau_{by}}{\tau_b} = \frac{\overline{V}}{\sqrt{\overline{U}^2 + \overline{V}^2}} \quad (24)$$

Chezy coefficient:

$$C_c = \frac{1}{n} R^{1/6} \quad (25)$$

The depth-averaged velocity and scalar quantity:

$$\overline{U} = \frac{1}{H}\int_{-h}^{\xi} U dZ$$

$$\overline{\phi} = \frac{1}{H}\int_{-h}^{\xi} \phi dZ \quad (26)$$

Mass conservation:

$$\frac{\partial(\overline{U})}{\partial x} + \frac{\partial(\overline{V})}{\partial y} = 0 \quad (27)$$

$$\overline{U}\frac{\partial \xi}{\partial x} + \overline{V}\frac{\partial \xi}{\partial y} = 0 \quad (28)$$

Momentum conservation:

$$\frac{\partial(H\overline{U}^2)}{\partial x} + \frac{\partial(H\overline{U}\overline{V})}{\partial y} = -gH\frac{\partial \xi}{\partial x} + \frac{1}{\rho}\frac{\partial(H\overline{\tau}_{xx})}{\partial x} + \frac{1}{\rho}\frac{\partial(H\overline{\tau}_{xy})}{\partial y} + \frac{\tau_{sx} - \tau_{bx}}{\rho} + \frac{1}{\rho}\frac{\partial}{\partial x}\int_{-h}^{\xi}\rho(U - \overline{U})^2 dZ + \frac{1}{\rho}\frac{\partial}{\partial y}\int_{-h}^{\xi}\rho(U - \overline{U})(V - \overline{V})dZ \quad (29)$$

$$\frac{\partial(H\overline{U}\overline{V})}{\partial x} + \frac{\partial(H\overline{V}^2)}{\partial y} = -gH\frac{\partial \xi}{\partial y} + \frac{1}{\rho}\frac{\partial(H\overline{\tau}_{yx})}{\partial y} + \frac{\tau_{sy} - \tau_{by}}{\rho} + \frac{1}{\rho}\frac{\partial}{\partial x}\int_{-h}^{\xi}\rho(U - \overline{U})(V - \overline{V})dZ + \frac{1}{\rho}\frac{\partial}{\partial y}\int_{-h}^{\xi}\rho(V - \overline{V})^2 dZ \quad (30)$$

The original form of Ph in Eqs.(12) and (13):

$$P_h = \overline{\nu}_t\left[2\left(\frac{\partial\overline{U}}{\partial x}\right)^2 + 2\left(\frac{\partial\overline{V}}{\partial y}\right)^2 + \left(\frac{\partial\overline{U}}{\partial y} + \frac{\partial\overline{V}}{\partial x}\right)^2\right] \quad (31)$$

Effective stresses:

$$T_{xy} = \frac{1}{H}\int_{-h}^{\xi}\left[\rho\nu\left(\frac{\partial\overline{U}}{\partial y} + \frac{\partial\overline{V}}{\partial x}\right) - \rho\overline{u'v'} + \rho(U - \overline{U})(V - \overline{V})\right]dz \quad (32)$$

$$T_{yy} = \frac{1}{H}\int_{-h}^{\xi}\left[2\rho\nu\frac{\partial\overline{V}}{\partial y} - \rho\overline{v'^2} + \rho(V - \overline{V})^2\right]dz \quad (33)$$

Water depth fluctuation:

$$\xi \doteq \left(\frac{Q}{\overline{U}B_e}\right) - h_0 \quad (34)$$

Turbulent viscosity coefficient:

$$\overline{\nu}_t = C_\mu\frac{\overline{k}^2}{\overline{\varepsilon}} \quad (35)$$

$\partial P/\partial x$ = Pressure gradient (36)

β^* = The pressure gradient parameter (37)

H_s = Shape factor = δ_*/δ_θ (38)

δ = boundary layer thickness = $0.37x/(R_x)^{1/5}$ (39)

$\delta_* = \frac{1}{8}\delta$ = mass displacement thickness (40)

$\delta_\theta = \frac{2}{72}\delta$ = momentum displacement thickness (41)

$R_x = U_1 x/\upsilon$: Reynold number at x distance from the upstream (42)

U_1 = the velocity profile at y=δ (43)

A. Primary velocity profile

What we consider here is the case of "rather large angle" between the walls so that the flow has the character of a central potential core and boundary layers along the walls. Only the self-similar boundary layer flow is considered, for which we assume the velocity distribution:

ISSN: 2277-3754
ISO 9001:2008 Certified
International Journal of Engineering and Innovative Technology (IJEIT)
Volume 4, Issue 3, September 2014

$$\frac{U(y)}{u_*} = \frac{1}{\kappa}\ln\left(\frac{9u_*y}{\nu}\right) - \frac{1}{\kappa}\left(\frac{y}{\delta}\right) \quad (44)$$

The distribution satisfies the boundary condition:

$dU/_{dy} = 0$ if $y = \delta$

When $y = \delta$, the core velocity, U_c is obtained from Eq.(44) as:

$$\frac{U_c(y)}{u_*} = \frac{1}{\kappa}\left[\ln\left(\frac{9u_*\delta}{\nu}\right) - 1\right] \quad (45)$$

The mean-velocity in the boundary, U_b, is seen to be:

$$\frac{U_b(y)}{u_*} = \frac{1}{\kappa}\left[\ln\left(\frac{9yu_*}{\nu}\right) - \frac{1}{2}\right] \quad (46)$$

Where κ is the von Karman constant in log law.

The mean velocity, $\overline{U(y)}$, over the entire half width, B_e, is:

$$\frac{\overline{U}(y)}{u_*} = \frac{U_c}{u_*} - 1.25\left(\frac{B_e}{\delta}\right), \quad (47)$$

The expression for the boundary layer, δ, is:

$$\frac{\delta}{B_e} = \frac{1}{|\beta|\left[\frac{1}{\kappa}\left(\frac{U_c}{u_*}\right) - 5.208\right]}; \quad \delta > 0, \quad (48)$$

where β is negative and in radius. Combining Eqs. (44) and (48), we have:

$$\frac{U(y)}{u_*} = \frac{1}{\kappa}\left[\ln\left(\frac{9yu_*}{\nu}\right) - \frac{\beta y\left(\frac{1}{\kappa}\frac{U_c}{u_*} - 5.208\right)}{B_e}\right] \quad (49)$$

Therefore, the mean-velocity over the entire half-width is:

$$\frac{\overline{U}(y)}{u_*} = \frac{1}{\kappa}\left[\ln\left(\frac{9B_eu_*}{\nu}\right) - 1 - \frac{\beta}{2}\left(\frac{1}{\kappa}\frac{U_c}{u_*} - 5.208\right)\right] \quad (50)$$

B. Turbulent shear stress profile

$$\frac{\tau_w}{\rho} = \frac{u_*^2(B_e - y)}{B_e^3}\left[y^2\left(27.12 + \frac{\beta^2}{\kappa^4}\right) + 10.42yB_e + B_e^2\left(\frac{10.42b^*}{\kappa^2} + 1\right)\right] +$$
$$\frac{u_*^2\beta y}{\kappa^4 B_e}\left[1 + \ln\left(\frac{9u_*y}{\nu}\right)\right]\left[\beta y\left(1 - \frac{2}{B_e}\right) + \beta y\ln\left(\frac{9u_*y}{\nu}\right) - 2\kappa^2\right](B_e - y) \quad (51)$$

This wall shear stress distribution is also agreeable for the condition that the shear stress vanishes on the centerline, $y = B_e$. When $y = 0$, by $L'Hospital'$s law, we obtain:

$$\left.\frac{\tau_w}{\rho}\right|_{y=0} = \left(\frac{10.42b^*}{\kappa^2} + 1\right)u_*^2; \quad b^* = \frac{|\beta|}{\left(\frac{1}{\kappa}\frac{U_c}{u^*} - 5.208\right)}; \quad (52)$$

The additive term in Eq.(52) is the wall shear stress due to rather large convergent core angle.

C. Turbulent viscosity coefficient

$$\nu_{ty} = \frac{(\tau_w/\rho)}{\left[\frac{\partial U(y)}{\partial y}\right]}$$
$$= -\frac{\kappa u_* y^2(B_e - y)\left(27.12 + \frac{\beta^2}{\kappa^4}\right)}{\beta B_e^2\left(\frac{1}{\kappa}\frac{U_c}{u_*} - 5.208\right)} - \frac{10.42\kappa u_* y(B_e - y)}{\beta B_e\left(\frac{1}{\kappa}\frac{U_c}{u_*} - 5.208\right)} \quad (53)$$

D. Dispersion Coefficient

$$U(y) - \overline{U}(y) = U'(y) \quad (54)$$

$$D_y = \frac{-1}{y}\int_0^y U'(y)\int_0^y \frac{1}{\nu_{ty}}\int_0^y U'(y)\,dydydy \quad (55)$$

$$D_y = \frac{u_*\beta^3}{2\kappa^3}B_e\left(\frac{y}{B_e} - \frac{1}{2}\right)\ln y\left[\frac{\left(\frac{1}{\kappa}\frac{U_c}{u_*} - 5.208\right)^3}{\left(27.12 + \frac{\beta^2}{\kappa^4}\right)}\right] + \frac{\beta^2 u_*}{\kappa^3}\left[\frac{\left(\frac{1}{\kappa}\frac{U_c}{u_*} - 5.208\right)^2}{\left(27.12 + \frac{\beta^2}{\kappa^4}\right)}\right) \cdot$$
$$\left(\frac{B_e^2}{y}\right)\left(\frac{y}{B_e} - \frac{1}{2}\right) - \frac{\beta^2 u_*}{2\kappa^3}\left[\frac{\left(\frac{1}{\kappa}\frac{U_c}{u_*} - 5.208\right)^2}{\left(27.12 + \frac{\beta^2}{\kappa^4}\right)}\right](B_e\ln y)\ln(y/B_e) +$$
$$-\frac{\beta^2 u_*}{2\kappa^3}\left[\frac{\left(\frac{1}{\kappa}\frac{U_c}{u_*} - 5.208\right)^2}{\left(27.12 + \frac{\beta^2}{\kappa^4}\right)}\right]B_e\ln y - \left(\frac{\beta u_*}{\kappa^3}\right)\left(\frac{B_e^2}{y}\right)\left[\frac{\left(\frac{1}{\kappa}\frac{U_c}{u_*} - 5.208\right)^2}{\left(27.12 + \frac{\beta^3}{\kappa^4}\right)}\right] +$$
$$-\left(\frac{\beta u_*}{\kappa^3}\right)\left[\frac{\left(\frac{1}{\kappa}\frac{U_c}{u_*} - 5.208\right)}{\left(27.12 + \frac{\beta^2}{\kappa^4}\right)}\right]\left(\frac{B_e^2}{y}\right)\ln y\left(\frac{y}{B_e}\right) \quad (56)$$

and:

$$\overline{D}_y = \frac{-1}{B_e}\int_0^{B_e} U'(y)\int_0^y \frac{1}{\nu_{ty}}\int_0^y U'(y)\,dydydy \quad (57)$$

ISSN: 2277-3754
ISO 9001:2008 Certified
International Journal of Engineering and Innovative Technology (IJEIT)
Volume 4, Issue 3, September 2014

$\overline{D}_y = -\frac{1}{B_e}\int_0^{B_e} D_y dy$, that is,

$$\overline{D}_y = \left(\frac{\beta^2 u_* B_e}{2\kappa^3}\right)\left[\frac{\left(\frac{1}{\kappa}\frac{U_c}{u_*} - 5.208\right)^2}{\left(27.12 + \frac{\beta^2}{\kappa^4}\right)}\right] - \left(\frac{\beta^3 u_* B_e}{8\kappa^3}\right)\left[\frac{\left(\frac{1}{\kappa}\frac{U_c}{u_*} - 5.208\right)^3}{\left(27.12 + \frac{\beta^2}{\kappa^4}\right)}\right] +$$

$$+\left(\frac{\beta u_* B_e}{\kappa^3}\right)(\ln B_e)^2\left[\frac{\left(\frac{1}{\kappa}\frac{U_c}{u_*} - 5.208\right)}{\left(27.12 + \frac{\beta^2}{\kappa^4}\right)}\right] + \left(\frac{\beta u_* B_e}{\kappa^3}\right)\left[\frac{\left(\frac{1}{\kappa}\frac{U_c}{u_*} - 5.208\right)^2}{\left(27.12 + \frac{\beta^2}{\kappa^4}\right)}\right](\ln B_e) +$$

$$-\left(\frac{2\beta^2 u_* B_e}{\kappa^3}\right)\left(1 - \frac{1}{2}\ln B_e\right)\left[\frac{\left(\frac{1}{\kappa}\frac{U_c}{u_*} - 5.208\right)^2}{\left(27.12 + \frac{\beta^2}{\kappa^4}\right)}\right] \tag{58}$$

E. Turbulent kinetic energy, $\bar{k}$:

$$\bar{k} = (1/2)(\overline{U'^2} + \overline{V'^2}) \tag{59}$$

where we have,

$$U(y) - \overline{U}(y) = U'(y) \tag{54}$$

$$V(y) - \overline{V}(y) = V'(y) \tag{60}$$

$$V = -\int\left(\frac{\partial U}{\partial x}\right)dy \tag{61}$$

$\overline{V}$ can be solved as the operation of Eq.(26)

For the purpose of simplification, the fluctuation item can be calculated by one-dimensional flow as in Eq. (34), and the convective item in y-direction momentum equation can be neglected by comparing to the one of x-direction:

$$\partial(HUV)/\partial x << \partial(HUV)/\partial y \tag{62}$$

F. Energy dissipation rate, $\overline{\varepsilon}$:

$$\overline{\nu}_t = C_\mu \frac{\overline{k}^2}{\overline{\varepsilon}} \tag{35}$$

Combining Eqs. (53) and (58), the value of energy dissipation rate can be solved.

IV. DISCUSSION AND CONCLUSIONS

A. The pressure gradient parameter

In the boundary layer flow, if the pressure gradient varies very large, the function of wake effect is affected for the smooth wall flows, but there is no function for the ones of rough wall. The pressure gradient parameter is the main factor, and is defined as Eq. (63), where τ0 is the bottom shear stress, rw is the specific weight of fluid, and H is the water depth along flow direction. For acceleration flow, dp/dx＜0, or β^*＜0, it means that the depth decreases along the x-direction; conversely, dp/dx＞0, or β^*＞0, the depth increases along the x-direction.

$$\beta^* = \frac{\delta_*}{\tau_0}\frac{dp}{dx} = \frac{\delta_*}{\tau_0}r_w\frac{dH}{dx} \tag{63}$$

B. The shape factor, H_s

H_s, shape factor, in Eq. (38), is a very important factor for the determination of friction factor, C_f. For dp/dx=0, then β^*=0, H_s has the maximum value at the upstream boundary, then it gradually reduce along the stream direction. The downstream has the H_s =1.3～1.5.(see Launder (9)).

If dp/dx＞0, then β^*＞0, so H_s increases until 2～3, then separation occurs. When dp/dx＜0, then β^*＜0, while H_s is almost the constant or say, H_s =1.1～1.2.

C. The friction coefficient, C_f

$$\frac{C_f}{2} = \left(\frac{u_*}{U_c}\right)^2 = 0.123\left(10^{-0.678H_s}\right)\left(\frac{U_c\delta_\theta}{\nu}\right)^{-0.268} \tag{64}$$

when dp/dx=0, or β^*=0, C_f could be solved from above equation with U_c and y=0.99δ, of course, u_* is got. If dp/dx＞0, or β^*＞0, H_s value is greater than the one of dp/dx=0, or β^*=0, then the C_f value is smaller than the one of dp/dx=0, or β^*=0. Consequently, C_f value of dp/dx＜0, or β^*＜0 will be greater than the one of dp/dx=0, or β^*=0 because of H_s of dp/dx＜0, or β^*＜0 smaller than the one of dp/dx=0, or β^*=0.

V. APPLICATIONS

A. The dispersion coefficient, $\overline{D}$

The dispersion coefficient related to mixing length coefficient will be used to express the situation of entrainment and the results of erosion or deposition of the channel bed. The dispersion coefficient or the mixing length coefficient is directly function of the variation of velocity along the flow direction, ∂U/∂x. From the ∂P/∂x =-U(∂U/∂x), the dispersion coefficient has the same trends as the trends of β^* and H_s .By the straightforward application of the dispersion coefficient in the unidirectional shear flow along the longitudinal flow direction (Tayler (10), Elder (11)) is, $\overline{D}$= 0.404hu_*/K, where K if function of von Karman constant. In the case of ∂P/∂x＞0, h is increasing along the flow, while decreasing along the flow with ∂P/∂x＜0. And the variation of water depth is much more evident than the one of shear velocity, u_*. Similarly, the turbulent viscosity coefficient has the same trends (Luo (12)). The variations of $\overline{D}$ for different β are shown in Fig. 1

B. The comparisons of boundary thickness, δ, and the centerline velocity between uniform and contraction flows:

Let h is the upstream water depth at the entrance of the converging wall flows, then the water level, H, is shown as H=h+ξ. Here ξ the fluctuation of water level is increasing along the flow direction with the decreasing of the boundary layer displacement, δ . By comparing the development of the boundary layer displacement of convergent wall flow, β＜0,

ISSN: 2277-3754
ISO 9001:2008 Certified
International Journal of Engineering and Innovative Technology (IJEIT)
Volume 4, Issue 3, September 2014

and the one of $\beta = 0$, we have the results in the following table (Table 1) with the given information:

$$r = (L - X)\sec\beta$$

$$L = B_0 \cot\beta \quad for\ \beta < 0$$

$$B_e = -(L - X)\tan\beta \tag{65}$$

The boundary layer displacements for these two cases show that they are almost the same magnitudes in the corresponding positions. By substituting δ into Eq. (45) to obtain U_c(y), we also can find that U_c is decreasing along the flow (see Table 2). By calculating the valve as follow for a givenβ, with the corresponding U_c(y) and B_e, as in Eq.(66), the B^*-value increases along the flow which results the decreasing of U_c(y). For a given discharge, the water level increases along the channel flow due to the decreasing of B_e and U_c(y) and Eq.(34) just gives us this information.

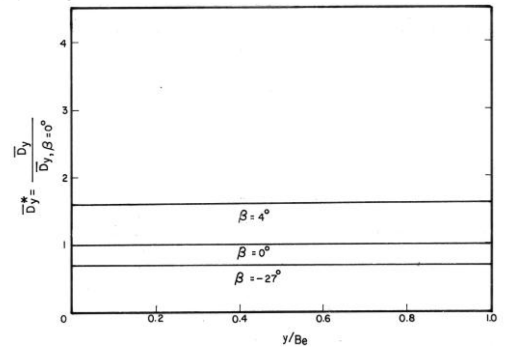

Fig. 1 Distributions of dimensionless dispersion coefficients value outside boundary for differentβ-value with B0＝5m, X＝10m, U0＝0.7m/s, friction velocity 0.050m/s, κ＝0.4, and h＝0.15m

Table 1 Comparisons of boundary layer thickness between uniform and convergent flows

B_0 = 5m, β = 0°; u_* = 0.05 m/sec; 20° C;				
x	5m	10	15	20
δ	0.08m	0.14	0.19	0.24
L = B_0cot β, β = -27°; u_* = 0.05 m/sec, 20°C				
L - X	5	10		
δ	0.10m	0.18		

$$\frac{\beta\left(\frac{1}{\kappa}\frac{U_c}{u_*} - 5.208\right)}{B_e} = B^* \tag{66}$$

Table 2 Changes of boundary layer thickness and centerline velocity along the contraction flow

B_e	2.5m	5m	B_e = -(L - X) tan β
δ	0.10m	0.18m	β = - 27°
U_c	1.21 m/sec	1.30 m/sec	u_* = 0.05 m/sec, T = 20°C

REFERENCES

[1] Rastogi A. K., Rodi W. (1978), Predictions of Heat and Mass Transfer in Open Channels, J. of the Hydraulics Division, ASCE, 104(3), 397–420.

[2] Chen Y.-S., Kim S.-M. (1987), Computation of Turbulent Flows using an Extended k- "Turbulence Closure Model, CR-179204, NASA, p. 21.

[3] Yakhot V., Orszag S. A., Thangam S., Gatski T. B., Speziale C. G. (1992), Development of Turbulence Models for Shear Flows by a Double Expansion Technique, Phys. Fluids A, 4(9).

[4] Flokstra C. (1977), The Closure Problem for Depth-Average Two Dimensional Flow, Publication No. 190, Delft Hydraulics Laboratory, The Netherlands.

[5] Wu W. (2004), Depth-Averaged 2-D Numerical Modeling of Unsteady Flow and Non-uniform Sediment Transport in Open Channels, accepted for publication by J. of Hydraulic Engineering, ASCE.

[6] Shyy W., Thakur S. S., Quyang H., Liu J., Blosch, E. (1997), Computational Techniques for Complex Transport Phenomenon, Cambridge University Press.

[7] Rodi W. (1993), Turbulence Models and Their Application in Hydraulics, 3rd Ed., IAHR Monograph, Balkema, Rottedam.

[8] Edward C. R. Luo (1993), Hydrodynamic Characteristics in Non-uniform Channel. Dissertation of Doctor, Asian Institute of Technology, Diss. No. WA 93-1.

[9] Launder, B. E. and Spalding, D. B. (1972), Mathematical Models of Turbulence, Academic Press, London, New York.

[10] Tayler, G. I. (1954, 1960), The Dispersion of Material in Turbulent Flow through a Pipe, Proc. R. Soc. London Ser. A223, pp. 446-468, also Sci Pap.2, pp. 466-488.

[11] Elder J. W. (1959), "The Dispersion of Marked Fluid in Turbulent Shear Flow", J. of Fluid Mechanics, Vol. 5, Part 4.

[12] Edward C. R. Luo (2013),"Hydrodynamic Characteristics of Expanded Channels with their Applications –the state-of-the-art", American Journal of Civil Engineering Vol. 1, No. 1, pp. 31-40.

AUTHOR BIOGRAPHY

Edward, C. R. Luo was born on 21, March 1957 in Taiwan. He has PhD degree in Business Administration Management, (PALLADIUM University, PALLAMA, 2004-2007) with major in Conflict and Strategic Management; PhD in Psychology (University of Central Nicaragua, NICARAGUA) with major in Theory and Practice on Psychotherapy and Counseling (2004-2007) and PhD in Hydrodynamics Engineering (1990—1993, Asian Institute of Technology, Thailand) with Major in River, Estuary, Marine, Ecological Engineering, and Debris Flow Engineering.
He has the following professional memberships as follow:2007 to now: Deputy Director General (DDG) of International Biographical Centre (IBC), Cambridge, England;2006 to now: Committee Member on Research and

ISSN: 2277-3754
ISO 9001:2008 Certified
International Journal of Engineering and Innovative Technology (IJEIT)
Volume 4, Issue 3, September 2014

Development of American Biographical Institute (ABI) U.S.A; Certified Licenses: EMF, International Engineers (Hydraulic Engineering); Asia-Pacific Engineers(Hydraulic Engineering); Senior Professional Hydraulic Engineer (P.E.), Taiwan; Arbitration Member, Taiwan.

Job Experience:

Jan. 2010 and continue, Chief Engineer of Hunghua Construction Co., Ltd. Taichung, Taiwan

Jan. 2001 and continue, Part-time Assistant Professor of National Chi Nan University, Nantou, Taiwan.

Sep.2010 to Aug.2013, Part-time Professor of Palladium University

Sep.2010 to Aug.2013, Part-time Professor of Southern Christian University

Sep.2010 to Aug.2013, Part-time Professor of University Central of Nicaragua

July 1997 to 2009, Chief Engineer, Hsing-Nan –Lung Construction Company

Jan. 2000 to Dec. 2006, President of Ching-Chan Eng. Ltd

Feb. 1994 to June 1995, Researcher, ITR

March 1984 to Dec. 1986, Advanced Engineer, WRB, MOE.

Aug. 1979 to Feb. 1984, Basic Engineer, WRB, MOE

Certified Licenses:

IPE, International Engineers（Hydraulic Engineering）

Asia-Pacific Engineers（Hydraulic Engineering）

Senior Professional Hydraulic Engineer (P.E.), Taiwan

Arbitration Member, Taiwan

Member on Quality Control, Taiwan

Senior Counselor in China, PRC

Senior Health Management Division in China, PRC

Senior Hydraulic Engineer in China, PRC

Senior Architect Engineer in China, PRC

Senior Municipal Utility Engineer in China, PRC

Senior Cost Analysis Engineer in China, PRC